IOPscience iopscience.iop.org

Home Search Collections Journals About Contact us My IOPscience

The exchange and correlation contribution to the electron - electron scattering part of the thermal resistivity in alkali metals

This article has been downloaded from IOPscience. Please scroll down to see the full text article.

1996 J. Phys.: Condens. Matter 8 1021

(http://iopscience.iop.org/0953-8984/8/8/013)

View the table of contents for this issue, or go to the journal homepage for more

Download details:
IP Address: 171.66.16.208
The article was downloaded on 13/05/2010 at 16:17

Please note that terms and conditions apply.

J. Phys.: Condens. Matter **8** (1996) 1021–1040. Printed in the UK

The exchange and correlation contribution to the electron–electron scattering part of the thermal resistivity in alkali metals

Lena Lundmark

Department of Theoretical Physics, University of Umeå, S-901 87 Umeå, Sweden

Received 23 October 1995

Abstract. We have calculated the pressure-dependent electron–electron scattering part of the thermal resistivity, $W_{ee}(P)$, for three alkali metals, Li, Na and K, using a Fermi liquid model. Within this model, the electron–electron interaction is given by self-energy derivatives. A first-order perturbation expansion of the self-energy Σ gives the commonly used GW-approximation. We have compared this with a $GW\Gamma$-approximation, where Γ is a vertex correction. By using a sum rule, we show that the $GW\Gamma$-approximation should be preferred in calculating the electron–electron interaction. We use four different static dielectric functions, describing the exchange and correlation, in the screening potential W, namely the RPA function, the SSTL function, an LDA function and a Hubbard modified version of the LDA function, HUB. We have also calculated the exchange and correlation contribution including *dynamic* dielectric functions, within the GW-approximation. The results for the sum rule indicate that the dynamic approximation that we use is not suitable for calculating the electron–electron interaction.

The thermal resistivity $W_{ee}(P)$ is calculated in the pressure region 0–120 kbar for Na and K, and in the region 0–100 kbar for Li. The LDA dielectric function gives results for $W_{ee}(P)$ for Li and K that are 10 to 20 times higher than the other dielectric functions, and also compared to experimental results. This has its origin in the approximation for the Γ function, which breaks down for small enough densities, when the electron density parameter is $r_s \geqslant 5$. The SSTL and Hubbard functions show quite similar behaviour for all three of the metals, except for at higher pressures in K ($\geqslant$100 kbar), where the SSTL function causes a more rapid increase in $W_{ee}(P)$. The RPA function, finally, gives a similar behaviour to the SSTL and Hubbard functions in $W_{ee}(P)$ for Na and K, while it results in a lowering of $W_{ee}(P)$ of $\approx$40% for Li.

We have also calculated the quasiparticle mass and the magnetic susceptibility, and compared these with experiment. Even in these cases it is the LDA function that gives the largest deviations from experiments.

1. Introduction

Even though the electron–electron scattering part of the thermal resistivity, W_{ee}, in metals only gives a minor contribution to the total thermal resistivity, it has intrinsic interest. It turns out to be one of the main causes for the deviation of the Lorentz function from the Wiedemann–Franz law above the Debye temperature, Θ_D. Laubitz [1] has managed brilliantly to separate this contribution from experimental total thermal and electrical resistivity results. Theoretically, W_{ee} can be calculated by solving the Boltzmann equation. It then turns out that the temperature dependence of W_{ee} is linear, $W_{ee} = BT$, where B is a constant. Several different approaches have been taken to calculate W_{ee}, giving results of the same order as experiments [2–4].

0953-8984/96/081021+20$19.50 © 1996 IOP Publishing Ltd

In an earlier paper, we calculated W_{ee} with particular emphasis on the pressure dependence for the alkali metals Li, Na and K [4]. We used an isotropic Fermi liquid model, as described by MacDonald and Geldart [2], and modified it in order to take account of the ions. The electron–electron interaction was described in terms of Landau parameters, given by Hedin [5], who used a simple *GW*-model, with the RPA screening function. The results at atmospheric pressure are within the experimental limits. Simple arguments show that the volume dependence is proportional to r_s^5, where r_s is the electron density parameter ($n = 4\pi r_s^3/3$). However, we have shown that taking account of the bandstructure of the metals, in terms of an effective band-mass, will give a more complex volume or pressure dependence [4].

We have also calculated the contribution from Umklapp scattering, which is an effect of the curvature of the Fermi surface, with particular emphasis on the pressure dependence [6]. This was first done by Lawrence and Wilkins [3], who followed a different approach in calculating W_{ee}. They used a variational method, where anisotropic scattering was also included. In their calculations, they were able to explicitly separate a contribution from Umklapp scattering. MacDonald and Geldart [2] incorporated this contribution into their calculations, showing that it only gives a minor correction at atmospheric pressure. We have shown that it also gives a minor correction to $W_{ee}(P)$ at higher pressures, of the order of $\sim$5% [6].

MacDonald and Geldart [2] have also calculated W_{ee} at atmospheric pressure using another set of Landau parameters given by Rice [7], who used a Hubbard model to describe the screening, proceeding from a different approach to that followed by Hedin [5]. These parameters gives values of W_{ee} that are $\sim$50% higher than the values given by Hedin's parameters, and also higher than the experimental results. This indicates the importance of the description of the electron–electron interaction itself, when calculating W_{ee}. Therefore, our aim within this paper is to investigate how exchange and correlation effects will affect W_{ee}, both at atmospheric and for higher pressures, when using different screening models, calculating the electron–electron interaction.

There has been a lot of interest in the electron–electron interaction in an electron gas for many years, and many different approaches have been followed within the many-body theory [5, 8–11]. Hedin [5] expressed the self-energy Σ in terms of the electron Green's function, $G(\boldsymbol{q})$, and a screened, static, potential, $W(\boldsymbol{q}) = v(\boldsymbol{q})/\varepsilon(\boldsymbol{q})$, where $v(\boldsymbol{q})$ is the Coulomb potential and $\varepsilon(\boldsymbol{q})$ is the dielectric screening function. The first term in a perturbation expansion of Σ is then given by *GW*, and the following terms will be of higher order in *W*. Including only the first term, *GW*, with a free-electron-like Green's function and a RPA dielectric function, Hedin arrived at a reduction of the occupied bandwidth of 5–10%, compared to the free-electron value in an electron gas.

Northrup *et al* [9, 10] have calculated the self-energy for Na, Li and Al using a method based on Hedin's *GW*-approximation. They include exchange and correlation effects in the screening dielectric function, $\varepsilon(\boldsymbol{q}, \omega)$, and approximate the dynamical dependence with a plasmon-pole model. The energy dependence of the Green's function was made consistent with the calculated quasiparticle energy spectrum. The self-energy gives a bandwidth reduction of 0.7 eV for Na, resulting in a total bandwidth of 2.5 eV, which is also the experimental value [9]. Using Hedin's method gave at most a reduction of 0.3 eV. The agreement in the case of Al is somewhat smaller, giving a bandwidth 6% too small [10], compared to experiment.

Mahan and Sernelius [11] argue that when using the *GW*-approximation, it is not consistent to include higher-order terms in the dielectric function, describing the exchange and correlation effects, as Northrup *et al* [9, 10] did, without including them in the *GW*-

approximation itself. Instead, one should work with a $GW\Gamma$-approximation, where Γ is the vertex correction. They show that this will decrease the bandwidth correction by 5–10%, compared to the GW-approximation. In the case of Na they obtain a bandwidth that is 10% too large [12], of the same size as Hedin's [5] results, but they argue that the experiments (photoemission) should be corrected for surface effects and broadening of electronic states, which would give better agreement with their results. In the case of Al, they get a bandwidth that is only 3% too large, which is better than what Northrup *et al* [10] achieved.

Within Landau's Fermi liquid theory, the quasiparticle interaction, $f(\boldsymbol{k}, \boldsymbol{k}')$, is given by the second-order derivative of the total energy of an electron gas with respect to the distribution function, $n_\sigma(\boldsymbol{k})$,

$$\delta E = \sum_{\boldsymbol{k},\sigma} \epsilon(\boldsymbol{k})\ \delta n_\sigma(\boldsymbol{k}) + \frac{1}{2} \sum_{\boldsymbol{k},\boldsymbol{k}',\sigma,\sigma'} f_{\sigma,\sigma'}(\boldsymbol{k}, \boldsymbol{k}')\ \delta n_\sigma(\boldsymbol{k})\ \delta n_{\sigma'}(\boldsymbol{k}') + \cdots \tag{1}$$

where

$$f_{\sigma,\sigma'}(\boldsymbol{k}, \boldsymbol{k}') = \frac{\delta\epsilon(\boldsymbol{k})}{\delta n_{\sigma'}(\boldsymbol{k}')} = \frac{\delta^2 E}{\delta n_\sigma(\boldsymbol{k})\ \delta n_{\sigma'}(\boldsymbol{k}')}. \tag{2}$$

E is here the total energy, $\epsilon(\boldsymbol{k})$ is the quasiparticle energy and σ is the spin index.

In this paper, we calculate $f(\boldsymbol{k}, \boldsymbol{k}')$ using both Hedin's GW-approximation [5] and Mahan and Sernelius's $GW\Gamma$-approximation [11], including different static dielectric functions in the screening potential. Expressing the interaction function in terms of Landau parameters, we check both approximations, using a sum rule. We also calculate $f(\boldsymbol{k}, \boldsymbol{k}')$ introducing the corresponding *dynamic* dielectric functions within the GW-approximation, using Overhauser's plasmon-pole model [13]. We then calculate the electron–electron scattering part of the thermal resistivity, using the Landau parameters, including the pressure dependence, for the alkali metals Li, Na and K. We also calculate the quasiparticle mass and the magnetic susceptibility for the alkali metals, and compare the results for different dielectric functions with experiments.

2. The quasiparticle interaction

The interaction function, $f(\boldsymbol{k}, \boldsymbol{k}')$, is calculated at the Fermi surface, which is assumed to be spherical. It then only depends on the angle θ between the $\boldsymbol{k}$-vectors. It is customary to split $f(\theta)$ into two functions, depending on the spin direction of the two interacting quasiparticles:

$$f_{\sigma,\sigma'}(\theta) = f_0(\theta) + f_e(\theta)\delta_{\sigma\sigma'}. \tag{3}$$

Following the notation used by Hedin and Lundqvist [8], we can write the interaction function as

$$f(\boldsymbol{k}, \boldsymbol{k}') = 2\pi \mathrm{i} Z^2 \frac{(2\pi)^3}{\Omega} \frac{\delta\Sigma(k)}{\delta G(k')} + Z \int \frac{\delta\Sigma(k)}{\delta G(q)}\ G^2(q)\ \frac{\delta\Sigma(q)}{\delta n_{k'}}\ \mathrm{d}\boldsymbol{q}\ \mathrm{d}\omega \tag{4}$$

where Z is the renormalization constant, $Z = (1 - \delta\Sigma/\delta\omega)^{-1}$, and Ω is the total volume of the system. $\Sigma(q)$ is the self-energy and *G(q)* is the Green's function. The notation q includes $(\boldsymbol{q}, \sigma, \omega)$, where ω is the quasiparticle energy.

The self-energy can be written in ordinary space as [5]

$$\Sigma(12) = \mathrm{i} \int W(1^+3) G(14) \Gamma(42; 3)\ \mathrm{d}(34) \tag{5}$$

where Γ is the vertex function. We have used the notation $(1) = (\boldsymbol{x}_1, t_1)$. The vertex function is given as

$$\Gamma(12;3) = \delta(12)\ \delta(13) + \int \frac{\delta\Sigma(12)}{\delta G(45)}\ G(46)G(75)\Gamma(67;3)\ \mathrm{d}(4567). \tag{6}$$

These two self-consistent equations will generate expressions for the self-energy as functionals of G in terms of the screened interaction W via an iteration process.

2.1. The static GW-approximation

If we only include the first term of Γ in Σ, and Fourier transform the expression, we arrive at

$$\Sigma(\boldsymbol{k},\omega) = \frac{\mathrm{i}}{(2\pi)^4}\int \mathrm{e}^{-\mathrm{i}\omega'\Delta} W(\boldsymbol{q},\omega')G(\boldsymbol{k}-\boldsymbol{q},\omega-\omega')\ \mathrm{d}\boldsymbol{q}\ \mathrm{d}\omega' \tag{7}$$

which is the commonly used GW-approximation. Δ is a positive increment, and we let $\Delta \to 0$ after performing the frequency integration.

Hedin [5] has calculated $f(\boldsymbol{k},\boldsymbol{k}')$ given by (4) in the GW-approximation. Including terms of the second order of the screened potential W, he obtained

$$\begin{aligned} f_e(\boldsymbol{k},\boldsymbol{k}') &= f_e^{(1)}(\boldsymbol{k},\boldsymbol{k}') + f_e^{(2)}(\boldsymbol{k},\boldsymbol{k}') \\ &= -\frac{Z^2}{\Omega}\left\{W(\boldsymbol{k}-\boldsymbol{k}';0) + \frac{\mathrm{i}}{(2\pi)^4}\int [2W(\boldsymbol{k}-\boldsymbol{k}';0)W(q)G(k+q)G(k'+q)\right. \\ &\quad \left. + W(q)W(q+k-k')G(k+q)(G(k'-q)+G(k+q))]\ \mathrm{d}\boldsymbol{q}\ \mathrm{d}\omega\right\} \end{aligned} \tag{8}$$

$$f_0(\boldsymbol{k},\boldsymbol{k}') = \frac{Z^2}{\Omega}\frac{\mathrm{i}}{(2\pi)^4}\int W^2(q)G(k+q)(G(k'-q)+G(k'+q))\ \mathrm{d}\boldsymbol{q}\ \mathrm{d}\omega. \tag{9}$$

He used a free-electron type of Green's function

$$G(\boldsymbol{q},\omega) = 1/(\omega - \epsilon_{|\boldsymbol{q}|} - \epsilon_0 - \mathrm{i}\delta_F) \tag{10}$$

where $\epsilon_{|\boldsymbol{q}|} = \hbar^2 q^2/2m$, $\delta_F > 0$ if $|\boldsymbol{q}| < k_F$ and $\delta_F < 0$ if $|\boldsymbol{q}| > k_F$. ϵ_0 was chosen as the correction to the chemical potential, $\mu = \epsilon_{k_F} + \epsilon_0$.

The screening potential, $W(\boldsymbol{q},\omega) = v(\boldsymbol{q})/\varepsilon(\boldsymbol{q},\omega)$, is then approximated in the statical limit, $W(\boldsymbol{q},0)$. The integration over ω in (8) and (9) is performed analytically, and the three-dimensional integration over $\boldsymbol{q}$ is computed numerically, for different values of the angle θ (the angle between $\boldsymbol{k}$ and $\boldsymbol{k}'$) and the electron density parameter, r_s.

Rice [7] has calculated the quasiparticle interaction from a different point of view. He used the definition of $f(\boldsymbol{k},\boldsymbol{k}')$ as the second derivative of the total energy with respect to the distribution function, equation (2). The energy was given by the Hubbard formula, and the derivation gave an expression of $f(\boldsymbol{k},\boldsymbol{k}')$ which looks very similar to the one given by Hedin. The main difference is the renormalization factor, Z, which does *not* occur in Rice's formula. Comparing results for the compressibility shows that the Z-factor should be excluded (see Hedin and Lundqvist [8]), so we have put $Z = 1$ in the rest of this paper.

2.2. The dynamic GW-approximation

The frequency dependence in the dielectric function, $\varepsilon(\boldsymbol{q},\omega)$, has been included by Northrup *et al* [10], and Hybertsen and Louie [14] using a plasmon-pole model, introduced by Overhauser [13]. They have calculated the self-energy in the GW-approximation using a

dynamically screened potential $W(\boldsymbol{q},\omega) = v(\boldsymbol{q})/\varepsilon(\boldsymbol{q},\omega)$. In the generalized plasmon-pole model, they postulate the dielectric function as

$$\varepsilon^{-1}(\boldsymbol{q},\omega) = 1 + A(\boldsymbol{q})[\omega - \tilde{\omega}(\boldsymbol{q}) + \mathrm{i}\delta]^{-1} - A(\boldsymbol{q})[\omega + \tilde{\omega}(\boldsymbol{q}) + \mathrm{i}\delta]^{-1} \tag{11}$$

where

$$A(\boldsymbol{q}) = -\frac{\pi}{2}\frac{\omega_p^2}{\tilde{\omega}(\boldsymbol{q})} \tag{12}$$

and the effective plasma frequency is given by

$$\tilde{\omega}^2(\boldsymbol{q}) = \omega_p^2/[1 - \varepsilon^{-1}(\boldsymbol{q})] \tag{13}$$

where ω_p is the ordinary plasma frequency. δ is here always positive.

We have used the plasmon-pole model to describe a dynamic dielectric function, calculating the quasiparticle interaction, $f(\boldsymbol{k},\boldsymbol{k}')$. We use the same equations as in the static case, (8) and (9), but we include the plasmon-pole model in the screened potential W. The frequency integral can still be evaluated analytically, and the $\boldsymbol{q}$-vector integration is then performed numerically. Details can be found in the appendix. The numerical calculations have to be performed with care, since the real part of the denominator is close to 0 in some regions in $\boldsymbol{q}$-space. This problem never occurs when calculating the self-energy, and it seems to have its origin in the plasmon-pole model itself.

2.3. The static GWΓ-approximation

Mahan and Sernelius [11] calculated the self-energy, including a vertex correction, Γ. The dominant, screening exchange part of the self-energy is then given by [15]

$$\Sigma(\boldsymbol{k},\omega) = \frac{\mathrm{i}}{(2\pi)^4}\int \mathrm{e}^{-\mathrm{i}\omega'\Delta} W(\boldsymbol{q},\omega')G(\boldsymbol{k}-\boldsymbol{q},\omega-\omega')\Gamma(\boldsymbol{q},\omega')\,\mathrm{d}\boldsymbol{q}\,\mathrm{d}\omega'. \tag{14}$$

They expressed the dielectric function as

$$\varepsilon(\boldsymbol{q},\omega) = 1 - v(\boldsymbol{q})P^0(\boldsymbol{q},\omega)\Gamma'(\boldsymbol{q},\omega) \tag{15}$$

with

$$\Gamma'(\boldsymbol{q},\omega) = 1/[1 + g(\boldsymbol{q})v(\boldsymbol{q})P^0(\boldsymbol{q},\omega)] \tag{16}$$

where $P_0(\boldsymbol{q},\omega)$ is the irreducible polarizability and $g(\boldsymbol{q})$ is a local-field correction. Several different approximations have been used to describe $g(\boldsymbol{q})$ [16–18]. It has been shown that the vertex correction is given by $\Gamma = \Gamma'$, for this type of dielectric function [19]. In this way, the self-energy will have the same power of the vertex correction Γ in the denominator and numerator of (14).

Proceeding from (14), the quasiparticle interaction is given by

$$\begin{aligned} f_e(\boldsymbol{k},\boldsymbol{k}') = -\frac{1}{\Omega}\Bigg\{ & W(\boldsymbol{k}-\boldsymbol{k}';0)\Gamma(\boldsymbol{k}-\boldsymbol{k}';0) \\ & + \frac{\mathrm{i}}{(2\pi)^4}\sum_\sigma \int \big[W(k-q)\Gamma(q)G^2(q)W(q-k')\Gamma(k') \\ & - v(q)g(q)W(q)\;\Gamma^2(q)G(k+q)(G(k'+q)+G(k'-q))\big]\;\mathrm{d}\boldsymbol{q}\;\mathrm{d}\omega\Bigg\} \end{aligned} \tag{17}$$

$$f_0(\boldsymbol{k},\boldsymbol{k}') = \frac{\mathrm{i}}{\Omega(2\pi)^4}\sum_\sigma \int \left\{W^2(q)\Gamma^3(q)G(k+q)(G(k'-q)+G(k'+q))\right\}\;\mathrm{d}\boldsymbol{q}\;\mathrm{d}\omega. \tag{18}$$

When the frequency integration is performed for a static, screened interaction, $W(\boldsymbol{q}, 0)$, and vertex function, $\Gamma(\boldsymbol{q}, 0)$, using a free-electron Green's function, and all quantities are made dimensionless, by multiplying by the factor $\Omega/(4\pi^2 e^2 \alpha r_s)$, we end up with the integrals

$$f_e(\boldsymbol{k}, \boldsymbol{k}') = -W'(\boldsymbol{k}-\boldsymbol{k}')\Gamma(\boldsymbol{k}-\boldsymbol{k}') + \frac{1}{\pi}\int W'(\boldsymbol{q})v'(\boldsymbol{q})\Gamma^2(\boldsymbol{q})g(\boldsymbol{q}) \times\left[\frac{\Theta_1}{(\boldsymbol{k}-\boldsymbol{k}')\cdot\boldsymbol{q}} - \frac{\Theta_2}{(\boldsymbol{k}-\boldsymbol{k}'+\boldsymbol{q})\cdot\boldsymbol{q}}\right] \mathrm{d}\boldsymbol{q} \tag{19}$$

$$f_0(\boldsymbol{k}, \boldsymbol{k}') = -\frac{1}{\pi}\int W'^2(\boldsymbol{q})\Gamma^3(\boldsymbol{q})\left[\frac{\Theta_1}{(\boldsymbol{k}-\boldsymbol{k}')\cdot\boldsymbol{q}} - \frac{\Theta_2}{(\boldsymbol{k}-\boldsymbol{k}'+\boldsymbol{q})\cdot\boldsymbol{q}}\right] \mathrm{d}\boldsymbol{q} \tag{20}$$

where $\boldsymbol{q}$, $\boldsymbol{k}$ and $\boldsymbol{k}'$ are in units of $2k_F$, and with the dimensionless quantities

$$W'(\boldsymbol{q}) = \frac{\alpha r_s}{4\pi|\boldsymbol{q}|^2\epsilon(|\boldsymbol{q}|)} \tag{21}$$

and

$$v'(\boldsymbol{q}) = \alpha r_s/4\pi|\boldsymbol{q}|^2 \tag{22}$$

with $\alpha = (4/9\pi)^{1/3}$. The step functions are defined as

$$\Theta_1 = \Theta(1/4 - (\boldsymbol{k}+\boldsymbol{q})^2) - \Theta(1/4 - (\boldsymbol{k}'+\boldsymbol{q})^2) \tag{23}$$

$$\Theta_2 = \Theta(1/4 - (\boldsymbol{k}+\boldsymbol{q})^2) - \Theta((\boldsymbol{k}'-\boldsymbol{q})^2 - 1/4). \tag{24}$$

The integrals (19) and (20) are then solved numerically.

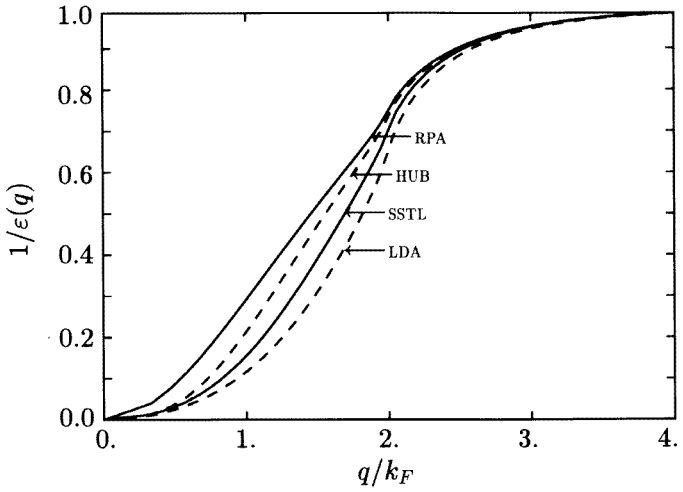

Figure 1. The four different dielectric functions, ε^{-1}, as functions of q/k_F, with $r_s = 4$. They are all given by (15) and (16), using different functions for $g(\boldsymbol{q})$, as described in the text.

2.4. The static dielectric functions

We have used four different static dielectric functions, corresponding to four different $g(\boldsymbol{q})$-functions in (16), to calculate $f(\boldsymbol{k}, \boldsymbol{k}')$. They are the RPA function, a function given by Singwi, Sjölander, Tosi and Land (SSTL) [16], an LDA function [18] and a Hubbard form of the LDA function (HUB). They are shown in figure 1, as a function of $\boldsymbol{q}$, for $r_s = 4$.

The RPA or Lindhard function, which is the simplest, corresponds to $g(\boldsymbol{q}) = 0$ in (16), which means that $\Gamma = \Gamma' = 1$, and we will not have any vertex corrections. It is derived by approximating the exact polarization diagram by its first term, the irreducible polarizability, $P^0(\boldsymbol{q}, 0)$.

The derivation of the SSTL dielectric function [16] explicitly includes screening effects from exchange and correlation holes in a parametrical form:

$$g^{SSTL}(\boldsymbol{q}) = a[1 - \mathrm{e}^{(-b|\boldsymbol{q}|^2/k_F^2)}] \tag{25}$$

where the parameters a and b depend on r_s.

The LDA dielectric function is obtained from the definition

$$g(\boldsymbol{q}) = -\frac{1}{v(\boldsymbol{q})}\frac{\delta V_{xc}}{\delta n} \tag{26}$$

where V_{xc} is the exchange and correlation potential and n is the charge density. We have chosen the parametrization given by Perdew and Zunger [18]:

$$g^{LDA}(\boldsymbol{q}) = -\frac{0.0474}{v(\boldsymbol{q})}\frac{r_s}{n(1 + 1.0529\sqrt{r_s} + 0.3334r_s)^3} \times\left(\frac{0.4387}{\sqrt{r_s}} + 0.8689 + 0.6143\sqrt{r_s} + 0.1482r_s\right) \tag{27}$$

where $n = \left(4\pi r_s^3/3\right)^{-1}$.

The Hubbard form, finally, is given by

$$g^{HUB}(\boldsymbol{q}) = g^{LDA}(\boldsymbol{q})\frac{k_F^2}{k_F^2 + |\boldsymbol{q}|^2} \tag{28}$$

where the correction to the LDA function corresponds to the original Hubbard model [17], which can be interpreted as a screening arising from the exchange hole around the electron.

The validity of these dielectric functions has been discussed by, e.g., Hedin and Lundqvist [8] and Mahan [15]. The SSTL function is argued to be preferred over the RPA and Hubbard functions, since it results in a positive pair distribution function (which it is by definition), while the other dielectric functions give a negative pair distribution function for small values of r, the electron–electron distance. The LDA version of $g(\boldsymbol{q})$ is quadratic in $\boldsymbol{q}$, while the other models give a $g(\boldsymbol{q})$ that is quadratic for small $\boldsymbol{q}$, and approaching an asymptotic value for large $\boldsymbol{q}$ (see figure 3 in [8]). However, the large-$\boldsymbol{q}$ behaviour of $g(\boldsymbol{q})$ is not crucial in the dielectric function, as $v(\boldsymbol{q})P^0(\boldsymbol{q})$ quickly drops to zero, outphasing the effect of $g(\boldsymbol{q})$.

2.5. Numerical calculations

The three-dimensional integrals in (19) and (20) and in the corresponding equations for the GW-approximation (equation (106) in Hedin [5]) were approximated as sums over all $\boldsymbol{q}$-vectors. The summation was performed in three orthogonal directions, finishing at $|\boldsymbol{q}| = 4k_F$. Symmetries allowed for restrictions in the number of $\boldsymbol{q}$-points used, and the quasiparticle interaction was well converged when the number of $\boldsymbol{q}$-points in each direction exceeded 100 within the given interval, i.e. with a spacing $<0.04k_F$ between the $\boldsymbol{q}$-points.

When using a dynamic dielectric function, the ω-dependent part of the integrals (8) and (9) is solved for analytically, ending up with the two three-dimensional integrals given in the appendix, equations (A1) and (A2). These are also solved numerically. The integrations have to be handled with care, since they will result in principal values which are close to

singularities. The problem occurs when $(\boldsymbol{q}-\boldsymbol{k}')\cdot\boldsymbol{q}=\tilde{\omega}'(\boldsymbol{q})$ in the denominator. The angle between $\boldsymbol{q}$ and $\boldsymbol{k}'$ is denoted as $\theta_{\boldsymbol{q}\boldsymbol{k}'}=a\cos\left(\boldsymbol{q}\cdot\boldsymbol{k}'\right)$. The real part of the denominator in the parentheses following the step function Θ_3 equals zero when the $\boldsymbol{q}$-vectors are positioned at an angle $\theta_{\boldsymbol{q}\boldsymbol{k}'0}$ relative to $\boldsymbol{k}'$ given as

$$\theta_{\boldsymbol{q}\boldsymbol{k}'0}\equiv a\cos\left(|\boldsymbol{q}|-\tilde{\omega}'(\boldsymbol{q})/|\boldsymbol{q}|\right). \tag{29}$$

In $f_e(\boldsymbol{k},\boldsymbol{k}')$, equation (A1), the denominator is linear, and in $f_0(\boldsymbol{k},\boldsymbol{k}')$, equation (A2), it is squared. The principal value has been handled in the following way: to every $\boldsymbol{q}$ we determine the corresponding $\theta_{\boldsymbol{q}\boldsymbol{k}'0}$ (if it exists). The integral is solved analytically for the azimuthal angular part, in a small area around the critical point, $\boldsymbol{q}_0$, with $\cos(\theta_{\boldsymbol{q}\boldsymbol{k}'0})\pm\alpha$, integrating over $\cos(\theta_{\boldsymbol{q}\boldsymbol{k}'})$, assuming the denominator of the integrand to be slowly varying in this region. α has been chosen to be 0.01 for the linear denominator, and 0.1 in the case of the squared denominator. With α equal to 0.1, the contribution from the analytical part of the integral is less than 1% of the total result, as explained in the appendix. When $\theta_{\boldsymbol{q}\boldsymbol{k}'0}$ is very close to 0 or π, we reduce the interval where the analytical solution is obtained, to make sure that we always have a symmetric interval around the critical angle. In that case, we solve for the part of the integral where $\cos(\theta_{\boldsymbol{q}\boldsymbol{k}'})$ is between the reduced interval and the original α numerically, by choosing the $\boldsymbol{q}$-points symmetrically around the critical angle. Those parts of the integral which are outside these regions are solved for as in the static case.

3. The Landau parameters

The quasiparticle interaction function $f(\boldsymbol{k},\boldsymbol{k}')$ can be expanded in terms of Legendre polynomials:

$$f_0(\boldsymbol{k},\boldsymbol{k}')+f_e(\boldsymbol{k},\boldsymbol{k}')/2=\sum_{l=0}^{\infty}(2l+1)F_l^s P_l(\cos\theta) \tag{30}$$

$$f_e(\boldsymbol{k},\boldsymbol{k}')/2=\sum_{l=0}^{\infty}(2l+1)F_l^a P_l(\cos\theta) \tag{31}$$

where θ is the angle between $\boldsymbol{k}$ and $\boldsymbol{k}'$. The Landau parameters F_l^s and F_l^a are then used to calculate W_{ee} as described in the next section.

The results for $f(\boldsymbol{k},\boldsymbol{k}')$ from using different models for the self-energy, Σ, and different dielectric functions can be checked by using the sum rule derived by Brinkman *et al* [20]:

$$S=1+\frac{F_0^a}{1+F_0^a}+\sum_{l=1}^{\infty}(2l+1)\left(\frac{F_l^s}{2l+1+F_l^s}+\frac{F_l^a}{1+F_l^a}\right)=0. \tag{32}$$

The results for the sum rule are given in table 1, for $r_s=4$. Using static dielectric functions, comparing the GW- and $GW\Gamma$-approximations, it turns out that the $GW\Gamma$-approximation gives results for S that are closer to 0 for all dielectric functions except the RPA one. However, since the RPA function is defined with $\Gamma=1$, the two approximations will be identical in this case. This indicates that the $GW\Gamma$-approximation should be used when including exchange and correlation in the dielectric function, as pointed out by Mahan and Sernelius [11].

With dynamical dielectric functions, we get results for the sum rule (using the GW-approximation) which are far from 0 for all dielectric functions, with the RPA giving the best result. The deviations seem to originate from the plasmon-pole model itself. As described by Overhauser [13], the excitation spectrum is replaced with a single mode, equation (13),

Table 1. Results for the sum rule, (32), obtained using two different expressions for the self-energy. The four columns show the results obtained when using four different dielectric functions, as described in the text. In the first row, we use the GW-approximation. The second row shows the corresponding results obtained using the $GW\Gamma$-approximation.

	RPA	SSTL	LDA	Hubbard
GW	0.3155	0.9788	1.0160	1.0453
$GW\Gamma$	0.3155	0.5568	0.7477	0.5757
Dynamic	4.5150	8.2328	6.5896	7.6941

where the plasmon mode dominates for small $\boldsymbol{q}$. This approximation is least reliable in the intermediate-$\boldsymbol{q}$ range, where the spectral width of the excitations is comparable to $\overline{h}\tilde{\omega}(\boldsymbol{q})$. It is in the same range that the denominators of the integrals, equations (A1) and (A2), become small, and it seems that the restrictions in the plasmon-pole model make it unsuitable for use when calculating the quasiparticle interaction.

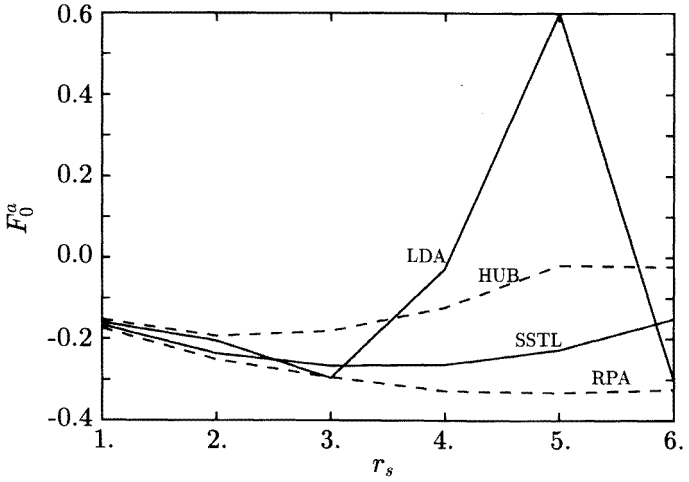

Figure 2. The Landau parameter F_0^a as a function of the electron density parameter, r_s. It was calculated using the $GW\Gamma$-approximation, including four different static dielectric functions: the RPA, LDA, and SSTL functions and a Hubbard form of the LDA function (HUB).

The Landau parameters F_0^a and F_1^s for the four different static dielectric functions are shown in figures 2 and 3, as functions of r_s, within the $GW\Gamma$-approximation. The parameters are larger in the dynamic case, as is shown in figures 4 and 5, particularly for large r_s-values. Three of the dielectric functions give quite similar r_s-dependence in the static case. The LDA function, however, gives rise to a rather peculiar behaviour of the parameters for large r_s, both in the static and in the dynamic case. This has its origin in a singularity in the approximated vertex function Γ, equation (16), and also in the dielectric function, when $g(\boldsymbol{q})v(\boldsymbol{q})P^0(\boldsymbol{q},0) = -1$, which occurs for a small, critical value of $\boldsymbol{q}$, when $r_s \geqslant 5$. Below this critical value of $\boldsymbol{q}$, $\Gamma(\boldsymbol{q})$ and $\varepsilon^{-1}(\boldsymbol{q})$ turn negative, and the result of the electron–electron interaction is then less reliable.

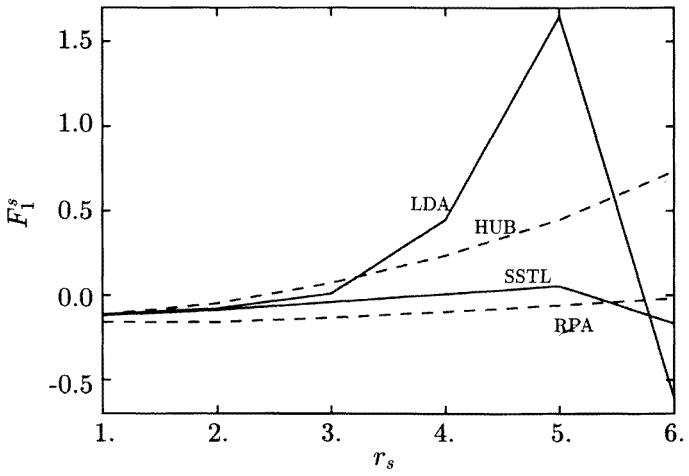

Figure 3. The Landau parameter F_1^s as a function of the electron density parameter, r_s. It was calculated using the $GW\Gamma$-approximation, including four different static dielectric functions: the RPA, LDA, and SSTL functions and a Hubbard form of the LDA function (HUB).

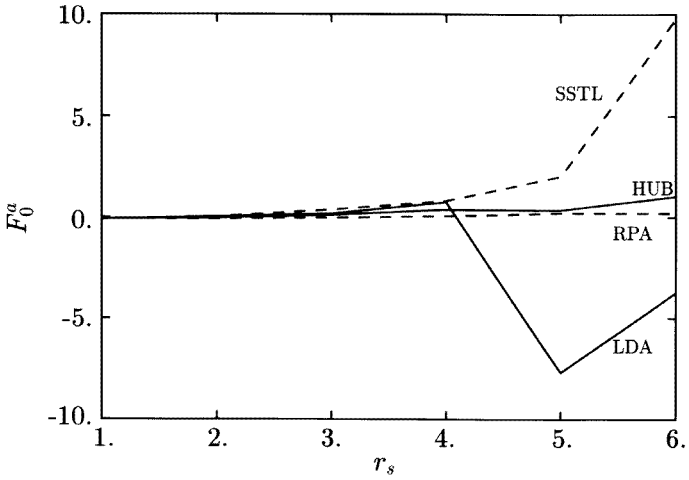

Figure 4. The Landau parameter F_0^a as a function of the electron density parameter, r_s. It was calculated using the GW-approximation, including four different dynamic dielectric functions: the RPA, LDA, and SSTL functions and a Hubbard form of the LDA function (HUB).

In turn, a negative dielectric function implies a negative compressibility function, which is defined from the relation

$$\lim_{q\to\infty} \varepsilon(\boldsymbol{q}, 0) = 1 + \left(\frac{q_{TF}}{|\boldsymbol{q}|}\right)^2 \frac{\kappa}{\kappa_{free}} \tag{33}$$

where q_{TF} is the Thomas–Fermi wave-number, and κ_{free} is the free-electron compressibility. A negative compressibility represents an unstable electron gas, and has been discussed in [8], [15] and [21]. This seems to be a result for all dielectric functions, when the density of the electron gas becomes smaller than a critical value, which differs slightly between different models. Gorobchenko *et al* [21] suggests that this 'is associated with the internal nature

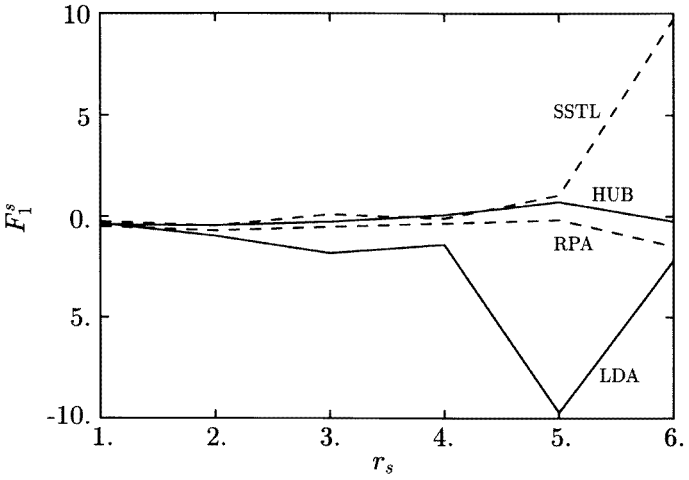

Figure 5. The Landau parameter F_1^s as a function of the electron density parameter, r_s. It was calculated using the GW-approximation, including four different dynamic dielectric functions: the RPA, LDA, and SSTL functions and a Hubbard form of the LDA function (HUB).

of the model under consideration and does not stem from the approximation used'. As a comparison with solids, it is noted that no metal exists with $r_s > 5.63$, which is the radius of Cs, indicating that there is a correspondence between unstable electron gases and solids.

As a check of the different dielectric functions, comparing with experimental results, we have calculated the quasiparticle mass, m^*, and the magnetic susceptibility, χ, for the alkali metals within the Fermi liquid model. The quasiparticle mass is given by

$$m^* = m_b(1 + F_1^s/3) \tag{34}$$

where the band-mass, m_b, has been calculated using an LMTO (linear muffin-tin orbital) bandstructure [4]. The Landau parameter used, F_1^s, is given for the four different dielectric functions, using the $GW\Gamma$-approximation in the static case, and the GW-approximation in the dynamic case.

Table 2. The quasiparticle mass, m^*, in units of the free-electron mass, as given by (34), for the three alkali metals Na, K and Li. In the first column, we give the effective radius, used for the Landau parameters. In the second column, the results obtained by using Hedin's GW-approximation, including the renormalization constant, Z, are shown. The next four columns show the results obtained using different dielectric functions, within the $GW\Gamma$-approximation. The last column shows experimental results, taken from the specific heat masses given by Kittel [22].

	r_s^*		Hedin	RPA	SSTL	LDA	Hubbard	Experiment
Na	3.72	Static	1.00	0.97	1.07	1.07	1.01	1.08 ± 0.04
		Dynamic	—	0.87	1.02	0.82	0.98	
K	4.55	Static	1.05	1.02	1.17	1.51	1.07	1.11 ± 0.03
		Dynamic	—	1.00	0.99	−1.22	1.24	
Li	5.00	Static	1.54	1.52	1.78	2.41	1.58	1.55 ± 0.15
		Dynamic	—	1.46	2.09	−3.47	1.92	

Since the Landau parameters are valid only for an electron gas, we have to take account of the ions in some simple way, when using the parameters for real metals. MacDonald and Geldart [2] have shown that one can simply rewrite the parameters as

$$\tilde{F}_l(r_s) = F_l(m_b r_s/\varepsilon) = F_l(r_s^*) \tag{35}$$

using an effective radius r_s^*, where ε is the dielectric constant given by $\varepsilon = 1 + 4\pi n\alpha$, n is the number density of the ions, and α is the polarizability of the individual ion cores. In the rest of the paper, we will always use the effective radius when we determine the Landau parameters for the different alkali metals.

The results for m^* at atmospheric pressure are given in table 2, for both the static and the dynamic case. We also include the results given by Hedin [5], including the renormalization constant, Z, in (8) and (9). A comparison with experimental results [22], where the electron–phonon renormalization was removed, is also included.

The results of the dynamic case are all deviating more from the experimental values than in the statical case. In particular, the LDA function gives an m^* that is *negative* for K and Li, showing no correspondence with experiments, indicating that the dynamical results are less reliable. The reason for these results is that the effective radius is in the region where the Landau parameters of the LDA function show a divergent behaviour.

Table 3. The magnetic spin susceptibility, χ, in units of the free-electron spin susceptibility, χ_0, as given by (36), for the three alkali metals Na, K and Li. In the first column, we give the effective radius used for obtaining the Landau parameters. In the second column, the results given by using Hedin's GW-approximation, including the renormalization constant, Z, are shown. The next four columns show the results obtained using different dielectric functions, within the $GW\Gamma$-approximation. The last column shows experimental results, given by Oliver and Myers [23].

	r_s^*		Hedin	RPA	SSTL	LDA	Hubbard	Experiment
Na	3.72	Static	1.15	1.44	1.46	1.30	1.18	1.67 ± 0.05
		Dynamic	—	0.84	0.58	0.32	0.73	
K	4.55	Static	1.19	1.53	1.55	1.07	1.13	1.73 ± 0.01
		Dynamic	—	0.86	0.52	0.39	0.92	
Li	5.00	Static	1.74	2.28	2.31	1.50	1.61	2.59 ± 0.06
		Dynamic	—	1.20	0.69	0.52	1.41	

Focusing on the static case, in the case of Na, the LDA and SSTL dielectric functions give results of m^* that are within the experimental limits, while the other functions give values of m^* that are too small. In the case of K and Li, the LDA function gives an m^* that is too high, again explained by the divergent behaviour of F_s^1. The SSTL function also gives values of m^* that are slightly too high for both K and Li. The other dielectric functions give values of m^* that are too small for K, while they are within the experimental limits for Li.

The spin magnetic susceptibility is given within the Fermi liquid model by

$$\frac{\chi}{\chi_0} = \frac{m^*}{m}\frac{1}{1+F_0^a} \tag{36}$$

where χ_0 is the free-electron magnetic susceptibility, and the quasiparticle mass, m^*, is given by (34). We have calculated the magnetic susceptibility at room temperature and atmospheric pressure using the four different Landau parameters, for the static and dynamic case, and the results are given in table 3. We have also compared with Hedin's results,

including the *Z*-constant. The experimental results are as given by Oliver and Myers [23], who calculated an experimental 'mean value', using the results from several experiments.

For all three of the alkali metals, all dielectric functions give values of χ that are too low, compared with experiment, in particular in the dynamic case. As with the quasiparticle mass, it is the LDA function that gives values of χ that deviate most from experiment, and the differences increase for larger effective radii. In the static case, the Hubbard function also shows large deviations. For all three of the metals, it is also clear that Hedin's results are much too low, indicating that the *Z*-constant should be put equal to 1.

4. The thermal resistivity and its pressure dependence

The thermal resistivity W_{ee} can be found by solving the Boltzmann equation, and for an isotropic Fermi liquid it is then given by [2]

$$W_{ee} = 2.622 \times 10^{-2}(m^{*2}r_s^5 T/H(\lambda))\langle\tilde{W}(\theta,\phi)(1-\cos\theta)/\cos(\theta/2)\rangle \qquad (37)$$

where $\langle\ldots\rangle$ denotes an surface integral over the spherical Fermi surface, i.e. over the angles θ and ϕ, which describes the relative location of four $\boldsymbol{k}$-vectors (all situated on the Fermi surface) representing the two interacting electrons before and after the scattering event, as explained by, e.g., Smith and Jensen [24]. $\tilde{W}(\theta,\phi)$ is the transition probability, m^* is the quasiparticle mass, given by (34), and $H(\lambda)$ is an infinite series that can be approximated to $\approx 1/2$.

The transition probability, $\tilde{W}(\theta,\phi)$, has been expanded in Legendre polynomials in the forward-scattering limit ($\phi = 0$), where the coefficients are simply related to the Landau parameters. If we include only two terms in the expansion of ϕ, we obtain

$$\tilde{W}_{\uparrow\uparrow} = |\tilde{A}_{\uparrow\uparrow}(\theta,0)\cos\phi|^2 \qquad (38)$$

$$\tilde{W}_{\uparrow\downarrow} = |\tfrac{1}{2}(2\tilde{A}_{\uparrow\downarrow}(\theta,0) - \tilde{A}_{\uparrow\uparrow}(\theta,0) + \tilde{A}_{\uparrow\uparrow}(\theta,0)\cos\phi)|^2 \qquad (39)$$

$$\tilde{A}_{\uparrow\sigma}(\theta,0) = 1 \pm \frac{F_0^a}{1+F_0 a} + \sum_l \left[\left(\frac{F_l^s}{1+F_l^s/(2l+1)} \pm \frac{F_l^a}{1+F_l^a/(2l+1)}\right)P_l(\cos\theta)\right] \qquad (40)$$

where the Landau parameters are modified according to (35).

Table 4. The electron–electron scattering part of thermal resistivity, W_{ee}/T, in units of 10^{-8} m W^{-1}, as given by (37), for the three alkali metals Na, K and Li. In the first column, we give the effective radius, used for obtaining the Landau parameters. In the second column, the results given by using Hedin's GW-approximation, including the renormalization constant, *Z*, are shown. The next four columns show the results obtained using different dielectric functions, within the $GW\Gamma$-approximation.

	r_s^*		Hedin	RPA	SSTL	LDA	Hubbard
Na	3.72	Static	67	73	65	85	69
		Dynamic	—	61	354	169	190
K	4.55	Static	231	244	270	4057	327
		Dynamic	—	400	895	43 100	1620
Li	5.00	Static	65	65	94	1633	101
		Dynamic	—	115	1490	28 900	570

We have calculated the pressure dependence of $W_{ee}(P)$ for three alkali metals, Li, Na and K. This was done earlier [4], using Hedin's Landau parameters, including the renormalization constant, *Z*, in (4). Now, we have instead used the Landau parameters

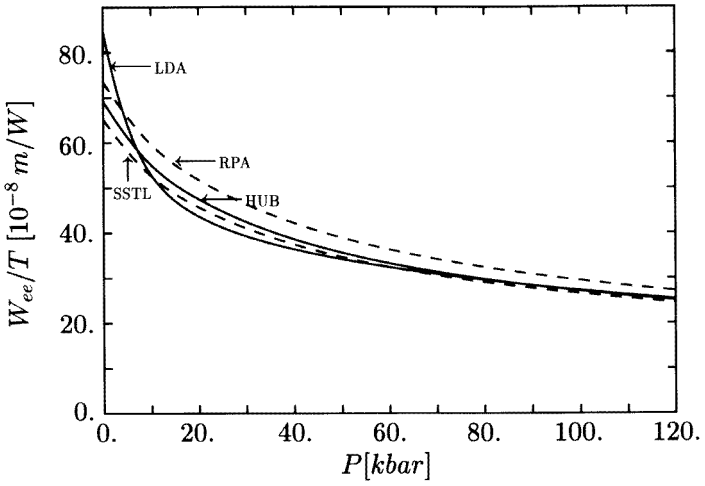

Figure 6. The pressure-dependent electron–electron scattering part of the thermal resistivity, $W_{ee}(P)/T$, in units of 10^{-8} m W^{-1} for Na, obtained using (37). We have used Landau parameters given by four different dielectric functions: the RPA, LDA, and SSTL functions and a Hubbard form of the LDA function (HUB).

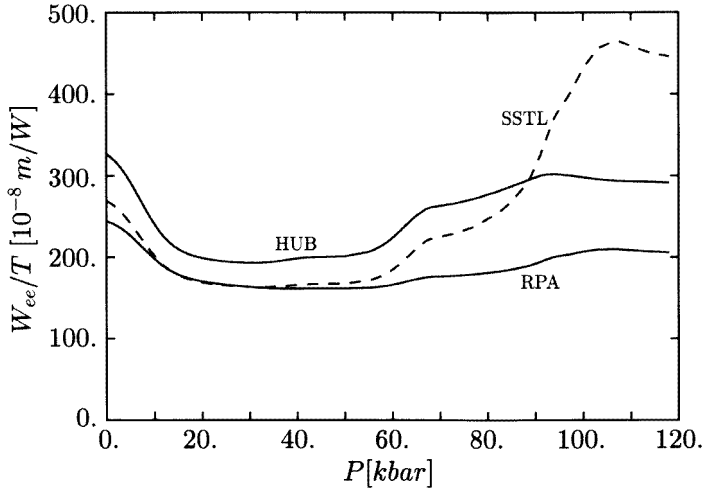

Figure 7. The pressure-dependent electron–electron scattering part of the thermal resistivity, $W_{ee}(P)/T$, in units of 10^{-8} m W^{-1} for K, obtained using (37). We have used Landau parameters given by three different dielectric functions: the RPA, and SSTL funtions and a Hubbard form of the LDA function (HUB).

given by the $GW\Gamma$-approximation, with the four different dielectric functions, in the static approximation. The results are shown in figures 6–8, where the pressure dependence is given by an equation of state. We also give the thermal resistivity at zero pressure, $W_{ee}(P = 0)$, in table 4, where a comparison with the dynamic case also is made. As the pressure dependence has been discussed more thoroughly in [4], we just point out a few important features here.

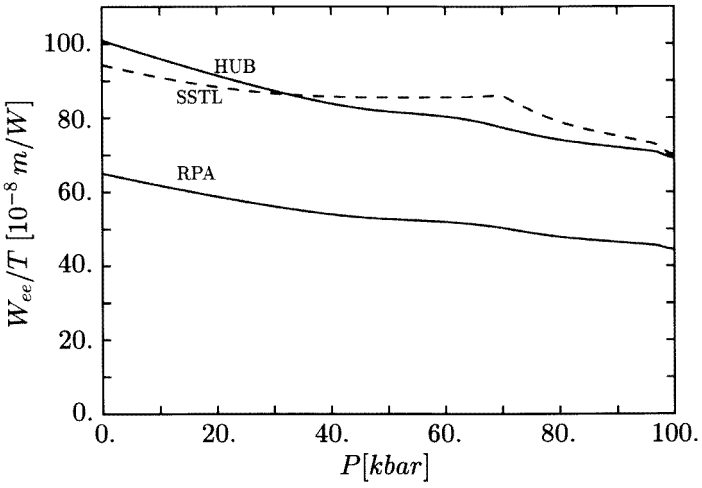

Figure 8. The pressure-dependent electron–electron scattering part of the thermal resistivity, $W_{ee}(P)/T$, in units of 10^{-8} m W^{-1} for Li, obtained using (37). We have used Landau parameters given by three different dielectric functions: the RPA, and SSTL functions and a Hubbard form of the LDA function (HUB).

First of all, if we neglect the effects of the bandstructure, the volume dependence will look like $W_{ee}(r_s) \sim r_s^5$. This is the case for Na, figure 6, which has an almost spherical Fermi surface. All dielectric functions give rather similar results for $W_{ee}(P)$, where the largest differences are at $P = 0$ kbar. The LDA function then results in a W_{ee} that is $\approx$25% larger than the lowest value, which is given by the SSTL function.

In the case of K, figure 7, the Fermi surface will be more distorted with increasing pressure, which means that the bandstructure will have a more prominent significance for the pressure dependence. This is most clearly seen in the band-mass, m_b. The thermal resistivity depends on the band-mass as $W_{ee} \sim m_b^2$, and m_b increases by almost a factor of 2 in the case of K [4], which is the reason for $W_{ee}(P)$ reaching a minimum and then starting to increase with increasing pressure. In figure 7 we show the results for $W_{ee}(P)$ obtained using the RPA, SSTL and Hubbard corrected LDA dielectric function (HUB). $W_{ee}(P)$ has the same pressure behaviour for these three dielectric functions, and they are relatively closely gathered at small pressures, spreading out more when the pressure is around 100 kbar, where the SSTL function gives the highest values, and the RPA the lowest one, with a difference of a factor of 2. The more rapid increase in $W_{ee}(P)$ using the SSTL function is mainly an effect of an increase in m^* (34), which can be seen in figure 2. In the pressure region of interest the effective radius is $4.3 \leqslant r_s^* \leqslant 5.4$, where the relative, absolute increase in F_s^1 is quite prominent for the SSTL function. Instead of describing the transition probability $\tilde{W}$ as a function of Landau parameters, it can of course also be rewritten as a function of m^* and χ, using the definitions (34) and (36). The increase in $\tilde{W}$ as a function of pressure can then also be described as being dominated by the increase in m^*. The LDA dielectric function, finally, not shown in figure 7, gives a $W_{ee}(P)$ which is more than 15 times larger than the other functions at $P = 0$, which is seen in table 4.

The displacement is even more pronounced in the case of Li, figure 8. Now, the results for different dielectric functions are more spread out, where the RPA function gives the lowest values of $W_{ee}(P)$, with the SSTL function and the Hubbard corrected LDA

function (HUB) in order of increase. The difference between the LDA function and the other dielectric functions at $P = 0$ kbar is now a factor of 25, according to table 4. Li has a more complex bandstructure than the other alkali metals, with a phase transition from bcc to fcc at 69 kbar, but the changes of the Fermi surface are not that dramatic in the pressure range of interest here, which means that the dominant part in $W_{ee}(P)$ is r_s^5, as in the case of Na.

A comparison between the static $GW\Gamma$-approximation and the dynamic GW-approximation of $W_{ee}(P = 0)$ in table 4, shows that the dynamic approximation gives larger values in all cases except for when using the RPA function for Na. This of course follows from the much larger values of the Landau parameters in the dynamic case, in particular for the higher effective radius, r_s^*.

Table 5. The quantity $W_{ee}/T - \rho_{ee}/L_0T^2$, in units of 10^{-8} m W^{-1}, for the two alkali metals Na and K, which is the quantity to be compared with experimental results. The Umklapp scattering function, Δ, and the DMR corrections have been included in W_{ee}. In the first column, the results given by using Hedin's GW-approximation, including the renormalization constant, Z, are shown. The next four columns show the results obtained using different dielectric functions, within the $GW\Gamma$-approximation. The last column shows experimental results, given by Cook and co-workers [25, 26].

		Hedin	RPA	SSTL	LDA	Hubbard	Experiment
Na	Static	78	84	75	98	80	110 ± 60
	Dynamic	—	70	408	195	220	
K	Static	261	275	305	4578	369	270 ± 50
	Dynamic	—	451	1011	48 600	1828	

A comparison with experimental data, which only are available at $P = 0$, gives a hint as to which dielectric function to prefer. The experimental results are given in table 5 for Na and K. MacDonald and Geldart [2] argue that the theoretical values of W_{ee} have to be corrected before any comparison with experiment can be made. One correction, which they refer to as a band correction, is expressed in a 'fractional Umklapp scattering' function, Δ. This will give a small increase of W_{ee}, of the order of a few per cent [6]. The second correction accounts for deviations from Matthiesen's rule (DMR), as an effect of the interference between electron–electron and electron–phonon scattering mechanisms. This correction will give an increase of W_{ee} of about 20%, according to MacDonald and Geldart [2].

Since the experimental value is calculated indirectly as the correction to the Lorentz function, given by the total electrical and thermal resistivity [1], the correct expression to compare with should be

$$\frac{W_{ee}}{T} - \frac{\rho_{ee}}{L_0T^2}. \tag{41}$$

Using MacDonald and Geldart's [2] expression for ρ_{ee}/L_0T^2, we arrive at the results given in table 5.

Using the static approximation, in the case of Na, all calculations are within the experimental limits, where the LDA dielectric function gives the highest value of W_{ee}, and the SSTL function gives the lowest value—very close to the results given by the RPA and Hubbard functions. The results for K are more spread out, and the value of W_{ee} obtained using the LDA function is far above the experimental limit. We have not calculated the corrected values for Li, since there are no experiments to compare with (at

least to our knowledge), but it is obvious that the LDA function will give a much higher value of $W_{ee}/T - \rho_{ee}/L_0T^2$ than the other functions. Since the RPA, SSTL and Hubbard dielectric functions show a rather similar behaviour of $W_{ee}(P)$ for all three alkali metals, it is impossible to select the best one. However, since the LDA dielectric function gives less correct values for K and deviates from the results given by the other dielectric functions for Li and Na, we can conclude that it gives less reliable results.

In general, the dynamical results deviate strongly from the experimental ones, ending up outside the experimental limits, in some cases even far outside the limits (as is the case with the LDA function for K). The only results that fit into the experimental limits are those obtained when using the RPA function for Na, with a result somewhat lower than in the static case. Using the RPA function, there is no difference between the GW- and $GW\Gamma$-approximation, since $\Gamma = 1$ in this case. However, the dynamical approximation seems to be less reliable, since in the case of K, the RPA function gives a result which is above the experimental limit.

5. Conclusions

The thermal resistivity W_{ee} is derived using the Fermi liquid model. Bandstructure effects are then included via the band-mass and a modified, effective electron radius, r_s^*. Describing a solid, this approximative way of taking care of the bandstructure will be most reliable for those alkali metals where the structure is most free-electron-like. The screening is described using four different dielectric functions, with both a static and a dynamic approximation. Calculating the electron–electron interaction, $f(\boldsymbol{k}, \boldsymbol{k}')$, we have shown, using a sum rule, equation (32), that the dynamic approximation gives results that are far from zero, the correct result. The reason for this is not obvious. It might be the dynamical approximation that is not useful in this case. In the static case, we have shown that a vertex correction should be included in the self-energy when a screening more complex than the RPA is used.

Since the calculations are based on the Fermi liquid model, the results for Na, which is most free-electron-like, should have the best correspondence with experiment. This is also true, at atmospheric pressure, where all static, dielectric functions give results for $W_{ee}(0)$ that are within the experimental limits. However, the differences are quite prominent, with the LDA function giving the largest value and the SSTL function the lowest value. With more accurate experiments, it would be possible to tell which of the screening functions to use, i.e. which function gives the most accurate description of the electron–electron interaction in this case.

The Fermi liquid model is less suitable for K, particularly at higher pressures, where the Fermi surface is rather disturbed, resulting in an increasing band-mass [4]. As a consequence, the thermal resistivity shows a minimum in the pressure interval. The results for the RPA and the Hubbard function are quite similar, while the SSTL function gives a more rapid increase for higher pressures. This is mainly caused by a rapidly increasing quasiparticle mass.

Li, finally, gives almost the same results for the SSTL and Hubbard functions, while the results for the RPA function are considerably lower. There are no experimental results for Li, which has a phase transition at low temperature, but for this case with a higher melting point than the other alkali metals, it would be possible to measure $W_{ee}(P)$ at room temperature. Such an experiment would give a lot of information concerning the different screening functions. The LDA function gives values of $W_{ee}(P)$ that apparently are unrealistic for both K and Li. These deviations are an effect of a singularity that occurs in the vertex function and dielectric function for high enough radius, $r_s \geqslant 5$.

Not surprisingly, from the poor results for the sum rule, the dynamic approximation gives results for $W_{ee}(P = 0)$ that agree less well with the experimental results, with deviations exceeding (in some cases very substantially) the experimental limits.

The quasiparticle mass and the spin magnetic susceptibility have also been calculated, expressed in Landau parameters, and compared with experiments. In the static case, we find that the LDA function is inadequate to reproduce the experimental values for high enough effective radius, $r_s^* > 4.5$, while the SSTL function gives the best agreement with the experimental values, even though the susceptibility is too low. In the dynamic case, the results usually deviate more from the experimental results, with the LDA function showing the largest deviations, which are in some cases rather unrealistic.

Acknowledgment

I am very grateful to Professor Arne Claesson for his support and continuous encouragement during this work.

Appendix

The three-dimensional integrals to be calculated, using a dynamic dielectric function, are given as

$$
\begin{aligned}
f_e(\boldsymbol{k},\boldsymbol{k}') = -W'(\boldsymbol{k}-\boldsymbol{k}') + \frac{1}{\pi}\int v'(\boldsymbol{q})\left\{\frac{2W'(\boldsymbol{k}-\boldsymbol{k}')}{(\boldsymbol{k}-\boldsymbol{k}')\cdot\boldsymbol{q}+\mathrm{i}\delta_e}\right.\\
\times\left[\Theta_1\left(1+\frac{\omega_p'^2}{((\boldsymbol{q}+\boldsymbol{k})\cdot\boldsymbol{q}+\mathrm{i}\delta_e)^2-\tilde{\omega}'^2(\boldsymbol{q})}\right)\right.\\
\left.\left.-\Theta_2\left(1+\frac{\omega_p'^2}{((\boldsymbol{q}+\boldsymbol{k}')\cdot\boldsymbol{q}+\mathrm{i}\delta_e)^2-\tilde{\omega}'^2(\boldsymbol{q})}\right)\right]\right.\\
-v'(\boldsymbol{q}+\boldsymbol{k}-\boldsymbol{k}')\left[\Theta_1\left(\frac{1}{(\boldsymbol{q}+\boldsymbol{k}-\boldsymbol{k}')\cdot\boldsymbol{q}+\mathrm{i}\delta_e}\right.\right.\\
\times\left(1+\frac{\omega_p'^2}{((\boldsymbol{q}+\boldsymbol{k})\cdot\boldsymbol{q}+\mathrm{i}\delta_e)^2-\tilde{\omega}'^2(\boldsymbol{q})}\right)\\
\times\left(1+\frac{\omega_p'^2}{((\boldsymbol{q}+\boldsymbol{k})\cdot\boldsymbol{q}+\mathrm{i}\delta_e)^2-\tilde{\omega}'^2(\boldsymbol{q}+\boldsymbol{k}-\boldsymbol{k}')}\right)+2\omega_p'^2((\boldsymbol{q}+\boldsymbol{k})\cdot\boldsymbol{q}+\mathrm{i}\delta_e)\\
\times\left(\left(1+\frac{\omega_p'^2}{\tilde{\omega}'^2(\boldsymbol{q})-\tilde{\omega}'^2(\boldsymbol{q}+\boldsymbol{k}-\boldsymbol{k}')}\right)\frac{1}{([(\boldsymbol{q}+\boldsymbol{k})\cdot\boldsymbol{q}+\mathrm{i}\delta_e]^2-\tilde{\omega}'^2(\boldsymbol{q}))^2}\right.\\
+\left(1-\frac{\omega_p'^2}{\tilde{\omega}'^2(\boldsymbol{q})-\tilde{\omega}'^2(\boldsymbol{q}+\boldsymbol{k}-\boldsymbol{k}')}\right)\\
\left.\left.\times\frac{1}{([(\boldsymbol{q}+\boldsymbol{k})\cdot\boldsymbol{q}+\mathrm{i}\delta_e]^2-\tilde{\omega}'^2(\boldsymbol{q}+\boldsymbol{k}-\boldsymbol{k}'))^2}\right)\right)\\
\left.-\frac{\Theta_3}{(\boldsymbol{q}+\boldsymbol{k}-\boldsymbol{k}')\cdot\boldsymbol{q}+\mathrm{i}\delta_e}\left(1+\frac{\omega_p'^2}{((\boldsymbol{q}-\boldsymbol{k}')\cdot\boldsymbol{q}-\mathrm{i}\delta_e)^2-\tilde{\omega}'^2(\boldsymbol{q})}\right)\right.
\end{aligned}
$$

$$\times \left(1 + \frac{\omega'^2_p}{((\boldsymbol{q}-\boldsymbol{k}')\cdot\boldsymbol{q} - \mathrm{i}\delta_e)^2 - \tilde{\omega}'^2(\boldsymbol{q}+\boldsymbol{k}-\boldsymbol{k}')}\right)\Bigg]\Bigg\}\,\mathrm{d}\boldsymbol{q} \tag{A1}$$

$$\begin{aligned} f_0(\boldsymbol{k},\boldsymbol{k}') = -\frac{1}{\pi}\int v'^2(\boldsymbol{q})\Bigg\{ & \frac{1}{(\boldsymbol{k}-\boldsymbol{k}')\cdot\boldsymbol{q} + \mathrm{i}\delta_0} \\ & \times\Bigg[\Theta_1\left(1 + \frac{\omega'^2_p}{((\boldsymbol{q}+\boldsymbol{k})\cdot\boldsymbol{q} + \mathrm{i}\delta_0)^2 - \tilde{\omega}'^2(\boldsymbol{q})}\right)^2 \\ & - \Theta_2\left(1 + \frac{\omega'^2_p}{((\boldsymbol{q}+\boldsymbol{k}')\cdot\boldsymbol{q} + \mathrm{i}\delta_0)^2 - \tilde{\omega}'^2(\boldsymbol{q})}\right)^2\Bigg] \\ & - \frac{1}{(\boldsymbol{q}+\boldsymbol{k}-\boldsymbol{k}')\cdot\boldsymbol{q} + \mathrm{i}\delta_0}\Bigg[\Theta_1\left(1 + \frac{\omega'^2_p}{((\boldsymbol{q}+\boldsymbol{k})\cdot\boldsymbol{q} + \mathrm{i}\delta_0)^2 - \tilde{\omega}'^2(\boldsymbol{q})}\right)^2 \\ & - \Theta_3\left(1 + \frac{\omega'^2_p}{((\boldsymbol{q}-\boldsymbol{k}')\cdot\boldsymbol{q} - \mathrm{i}\delta_0)^2 - \tilde{\omega}'^2(\boldsymbol{q})}\right)^2\Bigg]\Bigg\}\,\mathrm{d}\boldsymbol{q} \end{aligned} \tag{A2}$$

where $\boldsymbol{q}$, $\boldsymbol{k}$ and $\boldsymbol{k}'$ are in units of $2k_F$, and with the dimensionless quantities

$$\omega'^2_p = \frac{1}{3\pi}\left(\frac{9\pi}{4}\right)^{-1/3} r_s \tag{A3}$$

$$\tilde{\omega}'^2 = \omega'^2_p / \left[1 - \varepsilon^{-1}(\boldsymbol{q})\right] \tag{A4}$$

and where the step functions now are defined as

$$\Theta_1 = \Theta(1/4 - (\boldsymbol{k}+\boldsymbol{q})^2) \tag{A5}$$

$$\Theta_2 = \Theta(1/4 - (\boldsymbol{k}'+\boldsymbol{q})^2) \tag{A6}$$

$$\Theta_3 = \Theta((\boldsymbol{k}'-\boldsymbol{q})^2 - 1/4) \tag{A7}$$

and δ_e and δ_0 are infinite real numbers, originating from the Green function and the plasmon-pole model description of the dielectric function, (10) and (11), to avoid singularities. The principal value which is to be handled with care occurs in the term containing the step function Θ_3 in both $f_e(\boldsymbol{k},\boldsymbol{k}')$ and $f_0(\boldsymbol{k},\boldsymbol{k}')$ when $(\boldsymbol{q}-\boldsymbol{k}')\cdot\boldsymbol{q} = \tilde{\omega}'(\boldsymbol{q})$. In all other terms the step functions effectively exclude those $\boldsymbol{q}$-values where the small denominators occur.

The analytical solutions of the azimuthal angle parts ($\theta_{\boldsymbol{q}\boldsymbol{k}'}$) of the integrals (A1) and (A2) are given by expanding the denominator in a small interval, $\cos\theta_{\boldsymbol{q}\boldsymbol{k}'0} \pm \alpha$, around the critical point $\boldsymbol{q}_0$ and keeping the linear part only, according to

$$w(\boldsymbol{q}) \approx w(\boldsymbol{q}_0) + \frac{\mathrm{d}w(\boldsymbol{q}_0)}{\mathrm{d}\boldsymbol{q}}\cdot(\boldsymbol{q}-\boldsymbol{q}_0) \tag{A8}$$

where $w(\boldsymbol{q})$ represents the real part of the denominator, and $w(\boldsymbol{q}_0) = 0$. The validity of this approximation has been investigated by comparing the results for the two-dimensional integrals (of $|\boldsymbol{q}|$ and $\phi_{\boldsymbol{q}\boldsymbol{k}'}$) at the boundary between the analytical and numerical solution, i.e. at $\cos\theta_{\boldsymbol{q}\boldsymbol{k}'0} \pm \alpha$. We use both the exact expression of $w(\boldsymbol{q})$ and the linear approximation, equation (A8), in the last term of $f_0(\boldsymbol{k},\boldsymbol{k}')$, with a squared denominator. With $\alpha = 0.1$ the deviations between the analytical and numerical solutions at the boundary are 8% with $r_s = 1$, and 25% with $r_s = 6$, using the RPA dielectric function. However, the contribution from the analytical part to the total *three-dimensional* integral is $\leqslant$1%, indicating that the linear approximation will only have a minor effect on the final result.

References

[1] Laubitz M J 1970 *Phys. Rev.* B **2** 2252
[2] MacDonald A H and Geldart D J W 1980 *J. Phys. F: Met. Phys.* **10** 677
[3] Lawrence W E and Wilkins J W 1973 *Phys. Rev.* B **7** 2317
[4] Lundmark L 1988 *J. Phys. F: Met. Phys.* **18** 1855
[5] Hedin L 1965 *Phys. Rev.* **139** A796
[6] Lundmark L 1990 *J. Phys.: Condens. Matter* **2** 9309
[7] Rice T M 1965 *Ann. Phys.* **31** 100
[8] Hedin L and Lundqvist B I 1969 *Solid State Physics* vol 23 (New York: Academic) p 1
[9] Northrup J E, Hybertsen M S and Louie S G 1987 *Phys. Rev. Lett.* **59** 819
[10] Northrup J E, Hybertsen M S and Louie S G 1989 *Phys. Rev.* B **39** 8198
[11] Mahan G D and Sernelius B E 1989 *Phys. Rev. Lett.* **62** 2718
[12] Shung K W-K, Sernelius B E and Mahan G D 1987 *Phys. Rev.* B **36** 4499
[13] Overhauser A W 1971 *Phys. Rev.* B **3** 1888
[14] Hybertsen M S and Louie S G 1986 *Phys. Rev.* B **34** 5390
[15] Mahan G D 1990 *Many-Particle Physics* (New York: Plenum)
[16] Singwi K S, Sjölander A, Tosi M P and Land R H 1970 *Phys. Rev.* B **1** 1044
[17] Hubbard J 1957 *Proc. R. Soc.* A **240** 739; *Proc. R. Soc.* A **243** 336
[18] Perdew J P and Zunger A 1981 *Phys. Rev.* B **23** 5048
[19] Ting C S, Lee T K and Quinn J J 1974 *Phys. Rev. Lett.* **34** 870
[20] Brinkman W F, Platzmann P M and Rice T M 1968 *Phys. Rev.* **174** 495
[21] Gorobchenko V D, Kohn V N and Maksimov E G 1989 *The Dielectric Function of Condensed Systems* ed V M Agranovich *et al* (Amsterdam: North-Holland)
[22] Kittel C 1976 *Introduction to Solid State Physics* (New York: Wiley)
[23] Oliver C and Myers A 1989 *J. Phys.: Condens. Matter* **1** 9457
[24] Smith H and Jensen H H 1989 *Transport Phenomena* (Oxford: Oxford University Press)
[25] Cook J G, van der Meer M P and Laubitz M J 1972 *Can. J. Phys.* **50** 1386
[26] Cook J G 1979 *Can. J. Phys.* **57** 1216